

Electrochemical Determination of Alkaline Phosphatase as a Potential Marker of Reperfusion Injury

Shuang Qin^{1*}, Keshi Wang², Xinxin Ma³, Wangcheng Xiong¹, Zhongyi Yue¹ and Minliang Chen⁴

¹ Department of General Surgery, The First Affiliated Hospital of Xinxiang Medical College, Xinxiang, 453000, China.

² The First Clinical College, Xinxiang Medical College, Xinxiang, 453000, China

³ The Third Clinical College, Xinxiang Medical College, Xinxiang, 453000, China

⁴ First Affiliated Hospital, Chinese PLA Medical College, Beijing, 100048, P.R. China.

*E-mail: chenminliang98@foxmail.com

Received: 29 May 2017 / Accepted: 7 August 2017 / Published: 12 September 2017

Currently, there are no well-defined markers for distinguishing ischaemia from reperfusion injury. In this study, the practicality of a diagnostic health sensor was examined via the investigation of voltammetric alkaline phosphatase (ALP) detection. An indium tin oxide (ITO) film on glass was employed in the fabrication of an electrochemical sensor via facile photolithography using a transparent film and an office printer. The enzymatic hydrolysis of the substrate *p*-nitrophenyl phosphate (PNPP) by ALP produces *p*-nitrophenol, which was quantified by square wave voltammetry (SWV) and cyclic voltammetry (CV). Untreated human blood (UHB), human serum (HS), foetal bovine serum (FBS), and many other media provide a platform for ALP detection via this technique, which has a linear range of 5–250 U/L. The standard colorimetric analysis method was performed to further confirm the results.

Keywords: Alkaline phosphatase; Electrochemical sensor; Reperfusion injury; Electrode modification

1. INTRODUCTION

The immediate re-establishment of blood flow after an outbreak of intestinal ischaemia is essential for preventing irreversible anoxic tissue damage. Nevertheless, because oxygen free radicals are produced, further injury is caused by reperfusion. Until recently, no prominent marker has been available for distinguishing ischaemia from reperfusion injury. Arterial blood flow needs to be immediately re-established following abrupt intestinal ischaemia, which is death inducing. However, in addition to the preliminary ischaemia-related damage, more serious tissue-related damage may

follow as a result of the reperfusion itself. Reperfusion and ischaemia are undoubtedly two different processes, although differentiating their elements in intestinal damage is difficult. Intracellular adenosine triphosphate depletion, membrane disruption and homeostasis loss are caused by mitochondrial dysfunction affecting a range of cell activities and resulting in ischaemia-related injury [1, 2]. In contrast, in reperfusion injury, molecular oxygen is first reintroduced, which is mediated by neutrophils together with the oxygen free radicals that are produced by the xanthine oxidase enzyme system [3]. Herein, the significant vulnerability of alkaline phosphatase (ALP) activity to inactivation by free radical injury was exhibited in the intestinal brush border membranes of rats in an in vitro model of lipid peroxidation, as shown in our laboratory studies. In contrast, peptidases, disaccharidases and other integral brush border membrane enzymes could withstand free radical damage. Thus, novel ALP activity measurement-based experiments have been reported because the determination of ALP is remarkably important in clinical cases [4-7].

Furthermore, the fields of molecular biology and immunoassays have adopted it as a tracer [8-16]. Generally, enzyme-catalysed reactions feature amplified signals and high sensitivity, which are integrated with the specificity of antibody-antigen reactions that is embodied in enzyme immunoassays. Since ALP is inexpensive, highly productive, and remarkably stable, has wide substrate specificity, and is not sensitive to reaction interferences, the measurement of ALP activity has been widely adopted. The hydrolysis of orthophosphoric monoesters to alcohols can be achieved by the above enzyme, and its activity is detected via quantification of the produced alcohol. The majority of the extremely sensitive techniques [17-21] for ALP determination require extended incubation periods to attain their sensitivity. Therefore, reduction of the analysis period and simplification of the procedure are regarded as vital targets in the further development of standard analytical methods for diagnostics and industry, as well as for use in enzyme immunosensors.

Featuring innate resistance to organic adsorption and metal deposition, indium tin oxide (ITO) has gained widespread use as a conductive metal oxide [22]. Since ITO forms weak metal-oxide bonds, it only weakly adheres to metal adatoms [23]. Since its surface is minimally nucleophilic, ITO is resistive to the adsorption of organic molecules. ALP sensing also benefits from an advantage of ITO; since ITO is fully oxidized, it does not participate in any reactions at positive potentials. Specifically, at the potentials necessary to electrochemically analyse the most common ALP substrate, namely, PNPP, nearly no water oxidation current is observed. Based on these beneficial traits, ITO was chosen in this work as a potential material for an ALP sensor. An electrochemical sensor was fabricated from an ITO film on glass via facile photolithography using a transparent film and an office laser printer. The usefulness of this patterning technique is embodied not only in the construction of electrodes but also in the electrical connections of electrochemical sensors, where submicrometre-scale patterning is not necessary. Meanwhile, this patterning technique is also inexpensive and is convenient for preparing patterned conductive oxide films through a variety of methods, such as micro contact printing (μ CP) [24], inkjet printing [25] and photographic reduction [26], and many other inexpensive printing routes have been previously proposed as substitutes for photolithography. Only inexpensive tools and devices are needed to generate patterned ITO films by this method. With no need for chrome masks, this method is particularly suitable for biochemical and chemical laboratories that do not have access to the devices needed to generate photomasks that cater to microelectronics applications. To

generate patterns having functional microstructures with the desired traits, the continued development of a popular method was emphasized rather than proposing a novel technology. Laboratories that do not have access to devices for high-resolution printing or for constructing traditional chrome masks are able to construct micro-sized patterns via this technique.

This work proposes a combined sensor that contains the reference, counter and working electrodes on a single ITO plate. Using untreated human blood, human serum, FBS and many other media, ALP detection was achieved with adequately reproducible results. The results of medical standard colorimetric analyses conducted for comparison were used to further confirm the results.

2. EXPERIMENTS

2.1. Chemicals

The chemicals NaCl, $K_3[Fe(CN)_6]$, $FeCl_3$ and Ag_2SO_4 were purchased from Sigma. Alkaline phosphatase (ALP) and its substrates, including *p*-nitrophenol (PNP), dialyzed FBS (molecular cut off: 1000) and *p*-nitrophenyl phosphate disodium salt hexahydrate (PNPP), were obtained from Shanghai Reagent Co., Ltd. All materials were employed without further purification. Unless otherwise mentioned, triple-distilled water from a Modulab water system was employed for the preparation of aqueous solutions. All experiments were performed at ambient temperature.

2.2. Apparatus

All electrochemical measurements were controlled by a BAS 100B PC workstation with a triple-electrode configuration composed of a counter electrode (platinum wire), a reference electrode (Ag/AgCl), and a glassy carbon disk electrode or Au disk electrode. The SWV method was employed to quantitatively analyse ALP using a frequency of 25 Hz. Herein, ΔE_s equals 5 mV and E_{sw} equals 25 mV. Photolithography was achieved using an ultraviolet lamp (235-nm) and a homemade spin coating machine.

2.3. Sensor fabrication

The preparation process for the ITO microelectrodes is illustrated below. First, the ITO-coated glass was cleaned by sonication in methanol and acetone, followed by spin-coating of Su-8 photoresist on the ITO. Subsequently, light (235-nm) illumination was used to pattern the photoresist layer via a mask that was fabricated in a computer graphics programme. The photoresist was then developed, and the ITO surface was etched using an aqueous acid solution containing HNO_3 (5%) and HCl (20%) to transfer the pattern onto the substrate [27]. The residual photoresist was removed via sonication in a stripper solution. The dimensions and geometry of the ITO pattern was easily controlled by modifying the mask in the computer program. A resolution of approximately 50 μm was obtained for this technique.

3. RESULTS AND DISCUSSION

A minimum feature size of $\sim 50 \mu\text{m}$ was attained for the as-fabricated patterned ITO films. The reference, counter and working electrodes were combined on a single ITO plate since the ITO film could be easily patterned. The fabrication of these electrodes was achieved on a single piece of ITO. When connected to electronic appliances such as computers, the miniaturized ITO sensor can be applied in a variety of fields, and related experiments can be conveniently conducted since the sensor is fabricated in a facile approach. Prior to its use for ALP determination, a microelectrode with a $100 \mu\text{m}$ -wide band was subjected to CV analysis of a $\text{Fe}(\text{CNO})_6^{3-}/\text{Fe}(\text{CNO})_6^{4-}$ redox couple in aqueous solution. This work employed electrodes that were confirmed to be functional. The fabrication of the reference electrode (Ag/AgCl) on the surface of ITO is illustrated below. The construction began with electrodeposition of Ag on ITO via electrochemical reduction of Ag^+ in a Ag_2SO_4 solution. The reference electrode (Ag/AgCl) was installed on the ITO substrate by dipping the Ag-coated ITO electrode in an FeCl_3 solution (10 mM) for 0.5 min. These results also demonstrated that the electrode reaction of Cl^- at the electrode surface is a typical adsorption-controlled process. Figure 1 depicts the traits of the Ag/AgCl electrode, and those of a commercial reference electrode (Ag/AgCl) are shown for comparison.

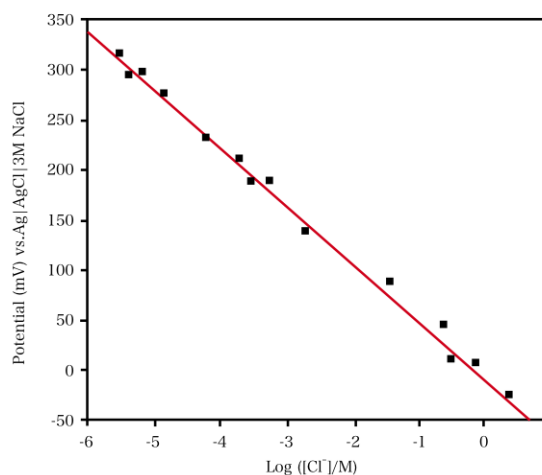


Figure 1. Change in the potential of the prepared reference electrode (Ag/AgCl) with different concentrations of Cl^- after dipping in an FeCl_3 solution (10 mM) for 0.5 min.

A linear potential versus $\log[\text{Cl}^-]$ was observed for the as-prepared reference electrode (Ag/AgCl). The slope of -54 mV/dec was consistent with the theoretical value of -56.7 mV/dec . In a sodium chloride solution (0.1 M), a potential variation of less than $\pm 3 \text{ mV}$ was obtained for more than 60 min. For a solution where the chloride ion concentration is known, the role of the reference electrode was effectively performed by the as-prepared solid-state Ag/AgCl electrode. Compared with reference electrodes on the market, the as-prepared reference electrode (Ag/AgCl) exhibited a steady potential in human whole blood, HS, FBS and many other media. A potential of approximately $+44 \text{ mV}$ was measured for the three media using the as-prepared solid-state electrode since bodily fluids contain similar chloride concentrations.

The adsorption of serum on different electrodes was studied as an initial confirmation. The electrode surface experienced non-specific adsorption due to the presence of serum albumin and numerous other organic adsorbent proteins in the serum. In addition to ITO, glassy carbon and Au were chosen because they are the most popular materials for electrodes. Since the rate of the ALP reaction depends on the substrate concentration, more sensitive biosensor responses should be obtained with large concentrations of phenyl phosphate [28-30]. However, as the phenyl phosphate concentration increased, a larger signal was observed from the spontaneous hydrolysis of the substrate. The adsorption is characterized in Figure 2, and the CV in FBS is provided in Figure 3A. Surface adsorption was observed for the glassy carbon electrode (GCE) and the Au electrode, though an electrochemical signal is not typically observed in FBS. A current was generated from the production of Au oxide and from its reduction at the Au electrode in addition to the current from adsorption. In contrast, a distinct current signal was not observed with the ITO electrode. Apart from a current of roughly +1.2 V that was caused by solution electrolysis, a clear baseline was observed. The effect of surface adsorption on electrochemical PNP oxidation was investigated using an FBS sample containing PNP (30 mM). Figure 2(B) depicts the peak current ratio for the oxidation of PNP vs. time. The peak current was observed to decline immediately with the GCE and the Au disk, as was predicted according to Figure 3(A). In contrast, the ITO electrode exhibited a stable current. Within approximately 5 min, the peak current stabilized and remained above 70% state for 30 min. These results confirm that ITO withstands adsorption. This improvement is due to the substantial amplification of the electrochemical signal achieved by graphite-TeXon composite enzyme electrodes, which allows the electrode to have a large amount of tyrosinase on its surface, maintain its activity, be in very close proximity to the transducer, and have a very good signal-to-noise ratio [31-33].

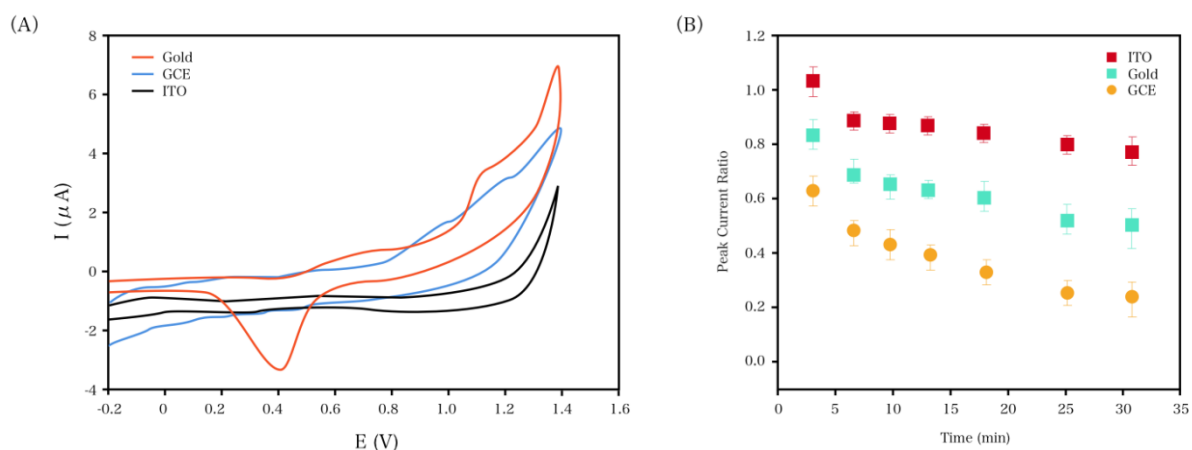


Figure 2. Comparison of surface adsorption to the different electrode materials in FBS: (A) CV in FBS and (B) the change in peak current vs. time in FBS containing 30 mM PNP ($\text{pH} = 7$).

Electrochemical analysis of ALP in HS and FBS, which are two distinct serums, was conducted using the ITO electrodes, and the results are indicated via the voltammograms in Figure 3. There is nearly no ALP in the FBS that was pretreated via dialysis on the material source, as indicated in Figure 3A. Since the FBS specimen contained little ALP, minimal change occurred when PNPP was added

into FBS. The absence of ALP is indicated by the nearly identical CVs for the PNPP-added FBS, represented by the dotted line, and the original FBS specimen, represented by the solid line. PNPP is enzymatically hydrolysed into PNP upon the addition of ALP into FBS, and the produced PNP is electrochemically detected. No obvious change was observed in either the response or the background current after ten regeneration/assay cycles. Thus, multiple samples can be determined using one electrode, dramatically increasing the sample throughput and reducing the sample analysis time [34]. In Figure 3A, the electrochemical oxidation of the hydrolysed PNP is depicted as the dashed line. A broad but clear peak was observed at +1.1 V. On the other hand, because HS contains a substantial amount of ALP, it was not necessary to add additional ALP to it. In the absence of ALP, PNPP was added into HS to generate PNP (Figure 4B). The ITO electrode is resistive to the adsorption of both HS and FBS despite their varying composition. The analytical behaviours were improved via SWV. The SWV results of the specimens are indicated in the insets of Figure 3A, and the CVs of the same specimens are shown in Figure 3B. Defined peaks a distinct baseline not impacted by solvent electrolysis were obtained from the SWV studies.

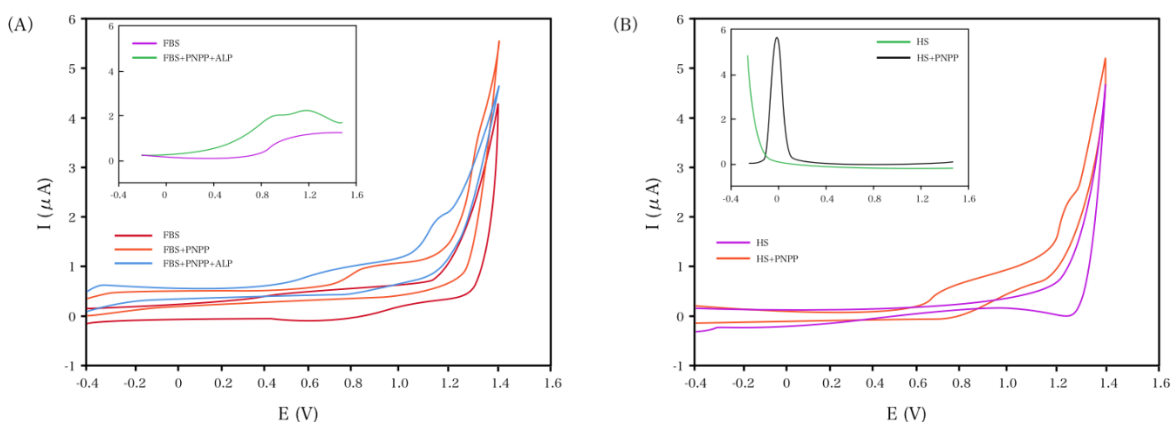


Figure 3. CVs from ALP detection in (A) FBS and (B) HS. The results obtained via square wave voltammetry under identical conditions are presented in the insets of each figure. Potential step increment: 5 mV; square wave amplitude: 15 mV; frequency: 20 Hz.

Figure 4 presents the characterization of the ALP activity quantification, where the relationships between (A) hydrolysis time and (B) ALP activity and the peak current for the hydrolysed PNP are indicated. Prior to the determination, the electrode was exposed to the blank serum for 5 min. An FBS specimen containing ALP (80 U/L) exhibited different peak currents for the various times, as indicated in Figure 4A. The peak current was proportional to hydrolysis time, with a value of 0.95 obtained as the correlation coefficient, r . After 20 min, the hydrolysis activity tended to decline even though there is a significant linear relationship between the hydrolysis time and peak current, which can be attributed to two issues. The influence of rising ALP activity in the system proposed here and in other short-term experiments has not been taken into consideration, even though this is a common research issue. Standard ALP additions were employed to investigate the relationship

between ALP activity and peak current, as shown in the results presented in Figure 5A. After each ALP addition, there was a 5 min period for hydrolysis with excess substrate, PNPP, to occur. A broad scope indicates the proportion of current response to activity, whereas in the case of elevated activity, a deviation from the correlation is observed. HS and FBS both have an identical linear dynamic range of 5–250 U/L for ALP based on the technique proposed herein. Based on the results of the SWV studies, a detection limit (DL) of 0.5 U/L was obtained for ALP activity, whereas a value of 3.6 U/L was obtained from CV. Since it is impractical for it to be applied if the sensitivity is lower than 1 U/L, 5 min was set as the hydrolysis time to achieve rapid determination, though the system provides better sensitivity with longer hydrolysis times. We compared the performance of this electrode with that of other ALP determination methods, as summarized in Table 1.

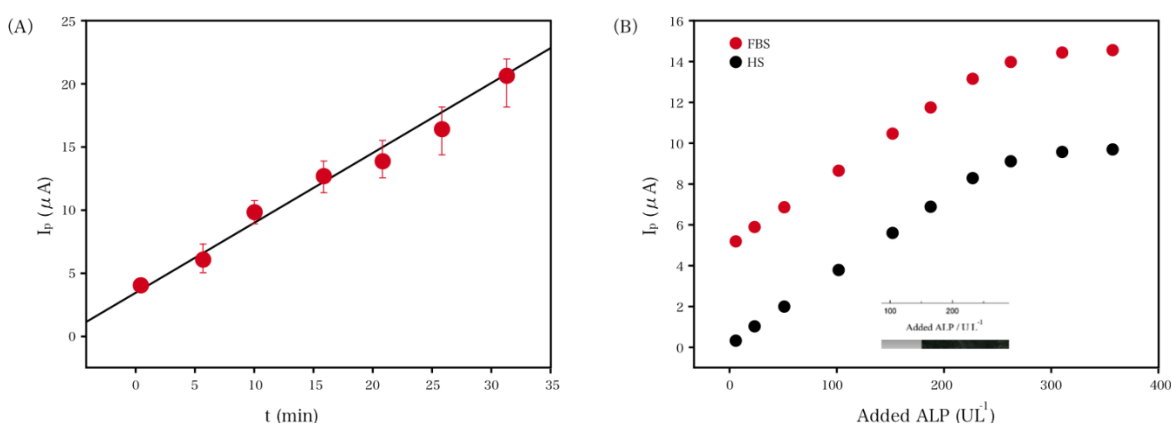


Figure 4. Comparison of surface adsorption to different electrode materials in FBS: (A) cyclic voltammograms in pure FBS and (B) change in the peak current with time in FBS containing 30 mM PNP.

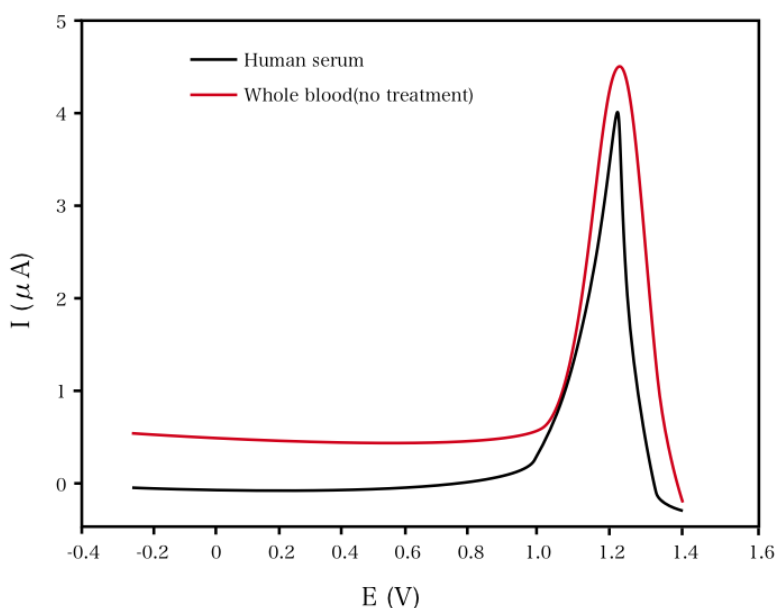


Figure 5. ALP detection in untreated human blood. Potential step increment: 5 mV; square wave amplitude: 15 mV; frequency: 20 Hz.

Table 1. ALP determination performance comparison between the proposed SWV determination method and other reports.

Detection method	LR	DL	Reference
Electrochemical Immunoassay	0.5-20	0.1	[17]
Western blots	—	—	[35]
Gold Nanoparticles	10-150 U/L	3 U/L	[36]
SWV	5–250 U/L	0.5 U/L	This work

To determine the selectivity of the proposed method, several other proteins, including HSA, BSA and Hb, were employed as controls. Although the concentrations of the other proteins were much higher than that of ALP, the decreases in their peaks were far less significant than those in the ALP assay. ALP in untreated human whole blood was employed for analysis due to the time-consuming process of constructing the ALP enzyme sensor, and the serum was prepared via centrifugation. The determination of ALP in the blood is illustrated below. The determination began with the addition of a concentrated PNPP solution (several drops) to fresh human blood. The mixture was hydrolysed for 5 min, followed by SWV analysis. The analysis of the human blood could be achieved before coagulation of the specimen since the maximum length of time needed to complete this method is 6 min. ALP determination in the whole blood and HS from the same person is indicated in Figure 5; the results are generally similar except for the wider peak whole blood. Hydrolysed PNP was colorimetrically detected via the standard medical approach, which contributed to the analysis of specimens. The results were compared with those from SWV analysis to confirm the strength of this electrochemical technique. Table 2 illustrates the results of the different methods for each specimen. The detection of ALP using the ITO-based sensor together with SWV was desirable because obviously similar results were obtained for the two techniques. Furthermore, in contrast to limit of the colorimetric approach to serum, this electrochemical technique can be conducted in not only whole blood but also HS.

Table 2. Comparison of the results from colorimetric and electrochemical determination.

	Colorimetric determination ALP activity (U/L)	Electrochemical determination
FBS	2.5	2.1
Human serum	90	89
Human blood	Not detectable	88

4. CONCLUSION

The integration of a micropatterned ITO sensor and square wave voltammetry presented was used to analyse ALP in serum and whole blood. Different patterns could be fabricated on ITO (50 μm resolution) via facile photolithography using a transparent film and an office printer. Untreated human blood, HS, FBS and many other media provide platforms for ALP detection based on the hydrolysis of the substrate, PNP phosphate, by ALP. A detection limit of 0.5 U/L was determined for ALP with a linear range of 5–250 U/L. With adequate reproducibility, this technique could be desirably applied. The standard colorimetric analysis method was conducted to confirm the results of the electrochemical method.

References

1. D. Parks and D. Granger, *American Journal of Physiology-Gastrointestinal and Liver Physiology*, 250 (1986) G749.
2. B. Zimmerman and D. Granger, *Surgical Clinics of North America*, 72 (1992) 65.
3. D. Parks, *Gut*, 30 (1989) 293.
4. W. Claeys, A. Van Loey and M. Hendrickx, *Trends in Food Science & Technology*, 13 (2002) 293.
5. V. Ximenes, A. Campa, W. Baader and L. Catalani, *Anal. Chim. Acta.*, 402 (1999) 99.
6. O. Bagel, B. Limoges, B. Schöllhorn and C. Degrand, *Anal. Chem.*, 69 (1997) 4688.
7. J. Lin, A. Tsuji and M. Maeda, *Anal. Chim. Acta.*, 339 (1997) 139.
8. Y. Che, Z. Yang, Y. Li, D. Paul and M. Slavik, *Journal of Rapid Methods & Automation in Microbiology*, 7 (1999) 47.
9. C. Nistor and J. Emnéus, *Analytical Communications*, 35 (1998) 417.
10. A. Benez, A. Geiselhart, R. Handgretinger, U. Schiebel and G. Fierlbeck, *Journal of Clinical Laboratory Analysis*, 13 (1999) 229.
11. Y. Che, Y. Li, M. Slavik and D. Paul, *Journal of Food Protection*, 63 (2000) 1043.
12. C. Ruan, H. Wang and Y. Li, *Transactions of the ASAE*, 45 (2002) 249.
13. M. Santandreu, F. Céspedes, S. Alegret and E. Martínez-Fàbregas, *Anal. Chem.*, 69 (1997) 2080.
14. C. Fernández-Sánchez and A. Costa-García, *Biosensors and Bioelectronics*, 12 (1997) 403.
15. E. Abad-Villar, M. Fernández-Abedul and A. Costa-García, *Anal. Chim. Acta.*, 409 (2000) 149.
16. C. Ruan and Y. Li, *Talanta*, 54 (2001) 1095.
17. C. Bauer, A. Eremenko, E. Ehrentreich-Förster, F. Bier, A. Makower, H. Halsall, W. Heineman and F. Scheller, *Analytical Chemistry*, 68 (1996) 2453.
18. L. Authier, B. Schöllhorn and B.t. Limoges, *Electroanalysis*, 10 (1998) 1255.
19. A. Díaz, F. Sánchez, M. Ramos and M. Torijas, *Sensors and Actuators B: Chemical*, 82 (2002) 176.
20. S. Ito, S. Yamazaki, K. Kano and T. Ikeda, *Anal. Chim. Acta.*, 424 (2000) 57.
21. M. Scintu, E. Daga and A. Ledda, *Journal of Food Protection*, 63 (2000) 1258.
22. J. Hsieh, T. Wu, J. Tong and Y. Yang, *Journal of Adhesion Science and Technology*, 17 (2003) 2085.
23. A. Davis and K. Dempsey, *Tetrahedron: Asymmetry*, 6 (1995) 2829.
24. T. Weskamp, V. Böhm and W. Herrmann, *Journal of Organometallic Chemistry*, 600 (2000) 12.
25. A. Kumar and G. Whitesides, *Applied Physics Letters*, 63 (1993) 2002.
26. T. Deng, H. Wu, S. Brittain and G. Whitesides, *Anal. Chem.*, 72 (2000) 3176.
27. M. Scholten and J. Van Den Meerakker, *Journal of the Electrochemical Society*, 140 (1993) 471.
28. C. Li, S. Zhen, J. Wang, Y. Li and C. Huang, *Biosensors and Bioelectronics*, 43 (2013) 366.
29. S. Dyhrman and B. Palenik, *Applied and Environmental Microbiology*, 65 (1999) 3205.

30. Z. Qian, L. Chai, Y. Huang, C. Tang, J. Shen, J. Chen and H. Feng, *Biosensors and Bioelectronics*, 68 (2015) 675.
31. B. Serra, S. Jiménez, M. Mena, A. Reviejo and J. Pingarrón, *Biosensors and Bioelectronics*, 17 (2002) 217.
32. L. Zhang, T. Hou, H. Li and F. Li, *Analyst*, 140 (2015) 4030.
33. C. Shen, X. Li, A. Rasooly, L. Guo, K. Zhang and M. Yang, *Biosensors and Bioelectronics*, 85 (2016) 220.
34. N. Xia, Y. Zhang, X. Wei, Y. Huang and L. Liu, *Analytica Chimica Acta*, 878 (2015) 95.
35. M. Blake, K. Johnston, G. Russell-Jones and E. Gotschlich, *Analytical Biochemistry*, 136 (1984) 175.
36. Y. Choi, N. Ho and C. Tung, *Angewandte Chemie International Edition*, 46 (2007) 707.

© 2017 The Authors. Published by ESG (www.electrochemsci.org). This article is an open access article distributed under the terms and conditions of the Creative Commons Attribution license (<http://creativecommons.org/licenses/by/4.0/>).